International Journal of Engineering Applied Sciences and Technology, 2018
Vol. 3, Issue 9, ISSN No. 2455-2143, Pages 31-36
Published Online January 2019 in IJEAST (http://www.ijeast.com)

ON HIGH TEMPERATURE MATERIALS: STRESS-RUPTURE CHARACTERISTICS OF AISI 310S STAINLESS STEEL SHEETS AT TEMPERATURE 973-1073K UNDER APPLIED STRESS 40-150MPa

A. Kanni Raj
School of Basic Sciences
Vel Tech Rangarajan Dr.Sagunthala R&D Institute of Science & Technology
Chennai, Tamil Nadu, India

Abstract— **Specimens of AISI 310S stainless steel sheets taken from the production runs of Salem stainless steel plant of Steel Authority of India limited were tested to failure under uniaxial tension. The plots of stress against rupture life were made to get stress exponent. The stress exponent, n, monotonically decreased as the temperature is increased. From the observed value of n (average 6.5), it can be said that the creep followed high temperature climb mechanism. The activation energy, Qc, is equal to 345kJ/mol which is larger than the activation energy for self-diffusion in pure FCC iron, i.e., 270-311kJ/mol. An activation energy of this magnitude indicates that the alloying elements in this steel are involved in the recovery climb process of the dislocation network. The creep master curve was also plotted for life prediction of high temperature components. Optical microscopic examination of stress-ruptured specimens revealed intergranular fracture, twin boundary formation, internal voids and cracks and branching internal cracks.**

Keywords— **Stress-rupture, creep, AISI 310S stainless steel, activation energy, intergranular fracture, Larson-Miller parameter**

I. INTRODUCTION

Creep is time dependent plastic deformation which may ultimately cause fracture. It is most likely to occur in components that are subjected to high loads at elevated temperatures. Design procedures are required to avoid excessive deformation and fracture in electric power generation equipment, aircraft gas turbine engines, chemical process plants, supersonic transport and space vehicle applications. The need for cost effectiveness and avoidance of failure is of paramount importance in all these industries [Rishiraj(2018), Maruyama et al.(2007), Voicu et al. (2009)].

Many parameters have been developed to predict long term creep properties from short term stress-rupture experiments. Also, several parameters which contain adjustable constants or parameters have been proposed to correlate rupture times (rupture lives) for different stress states. Damage tolerance is another parameter which is used to characterise the tolerance of a creeping material to stress concentrations. Many research works proved that alloys fail by cavitation and exhibit very little strain softening generally have damage tolerance values that lie between 1 and 1.25. A physically based approach for correlating intergranular cavitation and creep-rupture was proposed for materials that undergo grain boundary sliding [Kassner et al.(2000), Bano et al.(2014), Monteiro et al.(2017)].

The present dissertation has been undertaken to study the stress-rupture characteristics of AISI 310S stainless steel, an alloy used mainly for high temperature applications, in electrical energy production thermal power plant machinery such as boilers. The alloy in fully austenitised condition with coarse grain size of 100μm was subjected to stress-rupture studies. The tests were performed in air at test temperatures ranging from 973K to 1073K under an applied stress ranging from 40MPa to 150MPa.

II. MATERIALS & METHOD

The AISI 310S stainless steel sheets of dimensions 500mm X 500mm X 1.5mm were received from the stainless steel plant in the cold rolled and annealed condition. The chemical composition of the stainless steel sheet (in weight %) used in the present investigation was analysed by an emission spectrometer called Spectrovac (Model : ARL 3460 Metals

International Journal of Engineering Applied Sciences and Technology, 2018
Vol. 3, Issue 9, ISSN No. 2455-2143, Pages 31-36
Published Online January 2019 in IJEAST (http://www.ijeast.com)

Analyzer). Samples for optical microscopy were prepared following standard metallographic procedures, electrolytically etched using 10% Oxalic acid, and subsequently analysed under an optical microscope called Jenavert, with automatic light controlled photographic facility. The two-dimensional grain size was measured using Hayn intercept method. The sheets in the as-received condition had a grain size of 11μm (ASTM grain size number 10). A heat treatment procedure was adopted to produce specimens with a higher grain size number and a fully austenite structure. During heat-treatment, the specimens were solutionised by heating to 1323K and holding at the same temperature for 2 hours in a microprocessor controlled Eurotherm furnace (accuracy ±1K). Then the specimens were quenched in cold water to suppress carbide precipitation. A detailed heat treatment procedure is available elsewhere. After the heat treatment the samples contained grains with grain size 55μm (ASTM grain size number 5). These specimens were used for stress-rupture study. Room temperature tensile tests were conducted in a 250kN capacity Schenck Trebel electromechanical testing machine at a constant crosshead speed of 0.5mm/min (initial strain rate 0.00028/s) on ASTM E8M full size specimen prepared with tensile axis along the sheet rolling direction [Kanniraj(2007)]. The tensile properties such as 0.2% offset yield strength (YS), ultimate tensile strength (UTS) and total elongation (e_t) were obtained. The tensile testing is described in detail elsewhere. Vickers hardness (H_v) was evaluated on a Wolpert hardness tester as per ASTM standard. Load applied was 2kg and time of load application was 30s.

The stress-rupture experiments were conducted in Mayes high sensitivity constant load creep testing machine with a microprocessor control and self-adaptive temperature control on ASTM E8M subsize specimens, prepared with tensile axis along the sheet rolling direction [Kanniraj(2007)]. The machine is equivalent to a lever-beam type facility as developed by creep expert scientists, Andrade and Chalmers. The accuracy in the measurements are: load ±1N, temperature±1K and time ± 0.1h. The temperature was controlled by a Eurotherm controller, by PtRh-Pt thermocouple, with PID controler. The thermocouple junction was tied to the centre of the specimen using a nichrome wire. Load was applied in load cell attached to the specimen through a lever arm with lever ratio of 15 by universal coupling. The time was given by the elapsed timer attached to the machine. The machine was run in automatic condition for automatic maintenance of the specimen at the centre of the furnace by mercury level switches present in the lever. The rupture life (t_r) was shown by the elapsed timer which was automatically switched off by the weight of the lever. The experiment was repeated with three different temperature (T=973K, 1023K and 1073K) in the stress (σ) range 40-150MPa. A more detailed experimental procedure is given elsewhere [Kanniraj(2011,2013,2018), Decicco et al.(2005)]. Standard metallographic procedures were repeated on the stress-ruptured specimens to analyse the type of fracture and cracks.

III. Results & Discussion

Table-1 displays the chemical composition of AISI 310S stainless steel sheet. The room temperature mechanical properties of AISI 310S stainless steel sheets are given in Table-2.

Table-1 Alloying Elements (in weight percent) in AISI 310S stainless steel sheet.

C	Cr	Ni	Mn	Si	P	S
0.1	24.8	18.5	1.25	0.96	0.045	0.03

Table-2 Mechanical properties of AISI 310S stainless steel sheet.

*YS (MPa)	UTS (MPa)	^e_t	#H_v
204	516	42	192
* 0.2% Offset ^Gauge length 30mm # Load 2kg; time of load application 30s			

The mechanical properties are typical of fully annealed AISI 310 austenitic stainless steel sheet. Stress-rupture data of AISI 310S stainless steel sheets are presented in Table-3. The data can be analysed in terms of three common variables: rupture life, applied stress and test temperature. Other factors are also important, particularly, the fracture mode and deformation mechanism. However, for a straightforward presentation and representation of most experimental data, these three variables are sufficient. The time-to-ruptrure (rupture life, t_r) from isothermal stress-rupture testing is presented as a function of stress (σ) as follows:

$$t_r = k_1 e^{a\sigma} \quad (1)$$

where k_1 and a are constants, σ is the applied stress and t_r is the rupture life. The values obtained for k_1 and a in the present study are tabulated in Table-4. On the otherhand, the rupture life can be presented as a function of stress as follows:

$$t_r = k_2 \sigma^{-n} \quad (2)$$

where n is stress exponent and k_2 is a constant. The values obtained for stress exponent (n) and k_2 in the present study are given in Table-5. The stress exponent, n, monotonically decreased as the temperature is increased. A plot of rupture life against stress at 973K, 1023K and 1073K is presented in Fig.1. When temperature effects as well as stress effects on rupture life are to be considered, one common presentation is given by the following equation

$$t_r = k_3 \sigma^{-n} e^{-Qc/RT} \quad (3)$$

International Journal of Engineering Applied Sciences and Technology, 2018
Vol. 3, Issue 9, ISSN No. 2455-2143, Pages 31-36
Published Online January 2019 in IJEAST (http://www.ijeast.com)

where k_3 is a constant (k_3=0.000759h in the present case), n is stress exponent (n=6.5 in the present case), Q is the activation energy (Qc=345kJ/mol in the present case), R is the universal gas constant, T is absolute temperature and t_r is the rupture life.

Table-3 Stress-rupture data of AISI 310S stainless steel sheet.

T (K)	σ (MPa)	t_r (h)
973	75.80	326.5
	101.90	39.0
	102.65	41.1
	148.80	2.3
1023	66.60	86.2
	75.80	52.2
	86.50	15.4
	94.57	11.8
1073	41.97	209.9
	49.50	85.2
	59.70	31.5
	75.80	6.0
	86.50	2.9

Table-4 Numerical values of k_1 and a.

T (K)	k_1 (h)	a (m^2/N)
973	42812	$6.7x10^{-8}$
1023	14926	$7.7x10^{-8}$
1073	10989	$9.7x10^{-8}$

Table-5 Numerical values of k_2 and n.

T (K)	k_2 (h)	n
973	$2.4x10^{16}$	7.4
1023	$1.3x10^{13}$	6.2
1073	$1.3x10^{12}$	6.0

From the observed value of n (=6.5), it can be said that the creep followed high temperature climb mechanism in the temperature range 973-1073K. The activation energy, Qc, is equal to 345kJ/mol which is larger than the activation energy for self-diffusion (Qsd) in pure FCC iron, i.e., 270-311kJ/mol. An activation energy of this magnitude indicates that the alloying elements in this steel are involved in the recovery climb process of the dislocation network. The actvation energy (Qc) is independent of the applied stress for the present stress-rupture tests. Fig.2 shows the effect of temperature on rupture life at 75.8MPa and 86.5MPa.

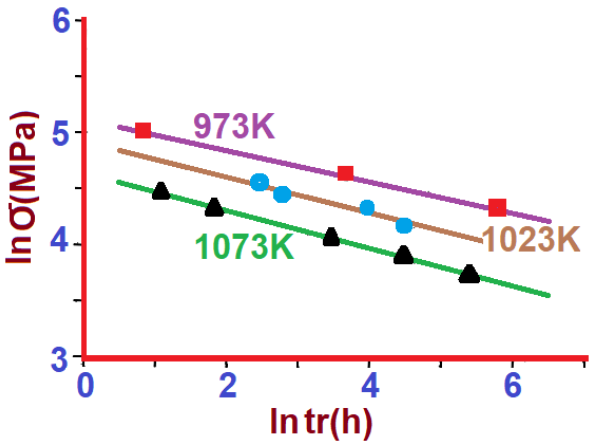

Fig.1. Plot of Rupture life as a function of applied stress at 973K, 1023K and 1073K.

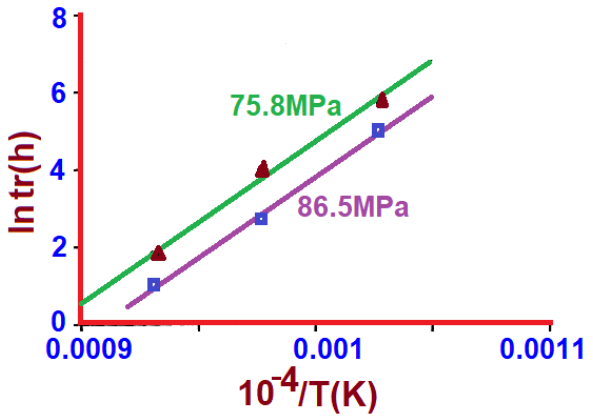

Fig.2. Effect of temperature on rupture life at applied stresses 75.8MPa and 86.5MPa.

Larson-Miller parameter (LMP) represents another approach using a single curve to represent data gathered under a variety of conditions. Larson-Miller parameter is given by

$$P_{LM}=T(C+\ln t_r) \qquad (4)$$

where C is a constant (=37 in the present case), T is absolute temperature and t_r is the rupture life in hours. C is obtained from Fig.3. Calculated values of Larson-Miller parameters are found in Table-6. Fig.4 is the master curve of Larson-Miller parameter for AISI 310S stainless steel sheet which is linear. The master curve plotted using short term stress-rupture data can be used for the prediction of long term creep properties. From the plot, Larson-Miller parameter can also be represented by

International Journal of Engineering Applied Sciences and Technology, 2018
Vol. 3, Issue 9, ISSN No. 2455-2143, Pages 31-36
Published Online January 2019 in IJEAST (http://www.ijeast.com)

$$P_{LM} = k_4 \ln\sigma + k_5 \quad (5)$$

where k_4 and k_5 are constants (k_4= -0.000147 and k_5= 10.433 in the present case) and σ is applied stress in MPa.

Table-6 Larson-Miller parameters for AISI 301S alloy at 973-1073K under 40-150MPa

T(K)	σ (MPa)	lnσ	P_{LM}
973	148.8	5.0027	36734
	101.9	4.624	39488
	102.65	4.6314	41556
	75.8	4.3281	39539
1023	94.57	4.5494	43317
	86.5	4.4602	44385
	75.8	4.3281	45350
	66.6	4.1988	40567
1073	86.5	4.4602	41004
	75.0	4.3175	42331
	59.7	4.0894	40750
	49.5	3.902	41538
	41.97	3.737	40294

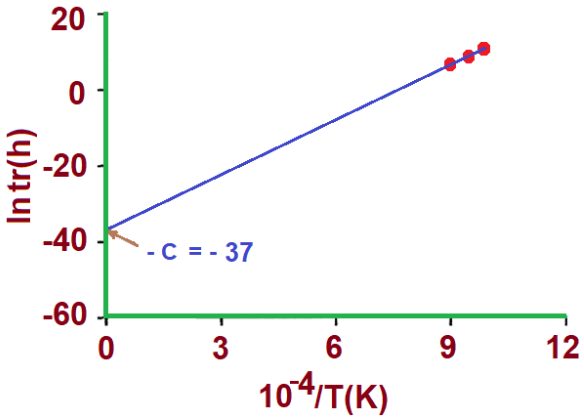

Fig.3. Effect of temperature on rupture life for stresses 75.8MPa to get C.

The design stresses evaluated from the Larson-Miller parameter method are tabulated for jet engine and steam turbine in the case of AISI 310S stainless steel (Table-7). Fig.5 shows the intergranular failure of crack initiation and propagation leading to fracture clearly noted even under low magnification. The optical micrograph is taken on the stress-ruptured specimen fractured after 11.8h at 1023K and 94.6MPa. Fig.6 is the enlarged view of stress-ruptured specimen after 86.4h at 1023K and 66.6MPa. Grain growth is noticeable. The close-up examination of stress-ruptured specimens revealed intergranular fracture, twin boundary formation, internal voids and cracks, wedge cracks and branching internal cracks.

Table-7 Design stresses evaluated based on Larson-Miller parameter

Engine	t_r(h)	Design stress, σ (MPa) for			
		973K	1073K	1173K	1273K
Jet	10000	46.5	23.6	11.98	6.08
Turbine	30000	39.7	19.8	9.90	4.95

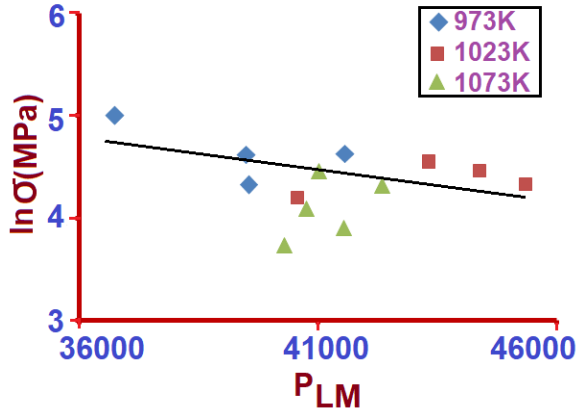

Fig.4. Master curve of Larson-Miller parameter for AISI 310S stainless steel sheet.

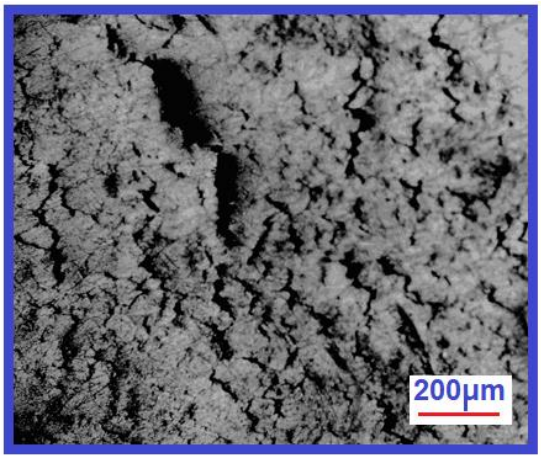

Fig.5. Optical micrograph of stress-ruptured specimen after 11.8h at 1023K and 94.6MPa.

In an earlier works, it has been reported wedge crack nucleation and growth in AISI 316 stainless steel as observed in the present study. From the microscopic observation analogous to that noted by Ashby and Dyson it could be possible to say that the damage tolerance values of AISI 310S stainless steel in the present test conditions lie between 1 and 1.25. Fig.7 is the stress-ruptured specimen after 41.1h at 973K and 102.7MPa which also shows internal crack. Fig.7 also shows twins typical of austenitic stainless steels and carbide precipitates. To understand its stress-rupture power, a

International Journal of Engineering Applied Sciences and Technology, 2018
Vol. 3, Issue 9, ISSN No. 2455-2143, Pages 31-36
Published Online January 2019 in IJEAST (http://www.ijeast.com)

comparison of stress-rupture plot of AISI 310S stainless steel was checked against that of AISI 600 super alloy. It was found from Fig.8 that the superalloy showed 3 times better resistance to stress-rupture [Taveres(2009)].

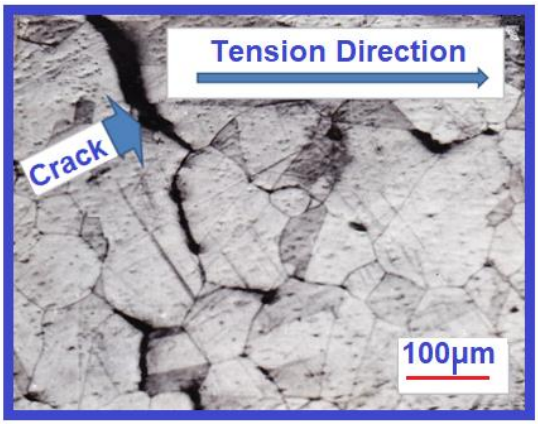

Fig.6. Optical micrograph of stress-ruptured specimen after 86.4h at 1023K and 66.6MPa.

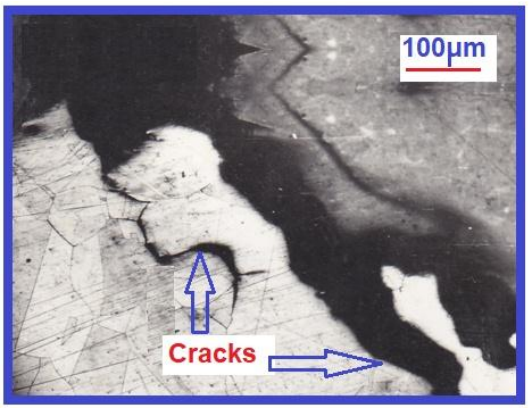

Fig.7. Optical micrograph of stress-ruptured specimen after 41.1h at 973K and 102.7MPa.

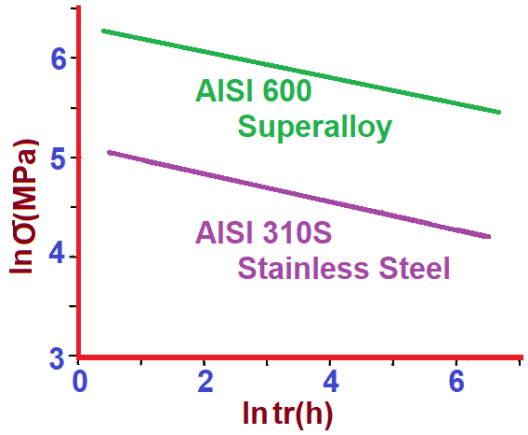

Fig.8. Stress-Rupture of AISI 310S stainless steel versus that of AISI600 Superalloy at 923K

IV. Conclusion

From the results obtained in the present study, the following conclusions have been derived.

(1) Stress exponent, n decreased as the temperature is increased (n values were 7.4, 6.1 and 6.0 respectively at 973K, 1023K and 1073K).
(2) From the observed value of n (average value of n=6.5), it can be said that the creep followed high temperature climb mechanism.
(3) The activation energy (Qc) obtained from logarithm rupture life-inverse temperature plot was 345kJ/mol.
(4) The Larson-Miller parameter master curve was linear with all the experimental points falling in a straight line.
(5) Metallographic examination supported intergranular fracture, branching internal cracks and wedge cracks.

V. References

[1] Rishiraj (2018). *Flow and fracture at high temperature. ASM International, Ohio, USA, ISBN - 9780871702012*

[2] Maruyama, K.; Ghassemi Armaki, H.; and Yoshimi, K. (2007). Multiregion analysis of creep rupture data of 316 stainless steel. *International Journal of Pressure Vessels and Piping*, 84, (pp.171–176)

[3] Voicu, R.; Lacaze, J.; Andrieu, E.; Poquillon, D.; and Furtado, J. (2009). Creep and tensile behaviour of austenitic Fe-Cr-Ni stainless steels. *Materials Science and Engineering A*, 510-511, (pp. 185–189)

[4] Kassner, M.E.; and Perez Prado, M.T. (2000). Five-power-law creep in single phase metals and alloys. *Progress in Materials Science*, 45, (pp. 1–102)

[5] Bano, N.; Koul, A.K.; and Nganbe, M. (2014). A deformation mechanism map for the 1.23Cr-1.2Mo-0.26V rotor steel and its verification using neural networks. *Metallurgical and Materials Transactions*, 45A, (pp.1928–1936)

[6] Monteiro, S.N.; Brandao, L.P.M., Paula, A. D. S.; Elias, C.N.; Pereira, A.C.; Assis, F. S. D.; Almeida, L.H.D.; and Araujo, L.S. (2017). Creep fracture mechanism and maps in AISI type 316 austenitic stainless steels from distinct origins.*Materials Research*, 20, (pp.892-898)

[7] Kanniraj, A. (2007). Room temperature formability of AISI 304 stainless steel sheets. *Manufacturing Technology Today*, 7 , (pp.15-20)

[8] Kanniraj, A. (2011). *Creep: Basic Theory and Dissertation. Lambert Academic Publishing, Saarbrucken, Germany, ISBN - 9783847303732*

[9] Kanniraj, A. (2013). On High-Temperature Materials: A Case on Creep and Oxidation of a Fully Austenitic Heat-Resistant Superalloy Stainless Steel Sheet. *Journal of*

Materials, Article ID-124649, http://dx.doi.org/10.1155/2013/124649, (pp.1-6)

[10] Kanniraj, A. (2018). On High Temperature Materials: An Overview of Deformation and Fracture Maps of a Super Alloy Stainless Steel by Analytical Modeling. *International Journal of Modern Engineering Research Technology*, 5, (pp. 222-230)

[11] De Cicco, H.; Luppo, M.I.; Raffaeli, H.; Di Gaetano, J.; Gribaudo, L.M.; and Ovejero-Garcia, J. (2005) Creep behavior of an A286 type stainless steel. *Materials Characterization*, 55, (pp.97–105)

[12] Tavares, S.S.M.; Moura, V.; da Costa, V.C.; Ferreira, M.L.R.; and Pardal, J.M. (2009). Microstructural changes and corrosion resistance of AISI 310S steel exposed to 600–800°C. *Materials Characterization*, 60, (pp.573–578)